

Supporting Information

Anti-Stokes Fluorescence Microscopy Using Direct and Indirect Dark State Formation.

Stefan Krause*, Miguel R. Carro-Temboury, Cecilia Cerretani and Tom Vosch*

Nanoscience Center and Department of Chemistry, University of Copenhagen, Universitetsparken 5, 2100 Copenhagen, Denmark. Email: stefan.krause@chem.ku.dk, tom@chem.ku.dk

Materials and Methods.

DNA encapsulated silver nanoclusters were synthesized and purified as described by Cerretani et al.¹ Briefly, the DNA-AgNCs have an absorption and emission maximum of 573 nm and 640 nm, respectively, in a 10 mM NH₄OAc solution at 25°C. At this temperature, the fluorescence quantum yield is 0.8 and the intensity-weighted average decay time is 2.59 ns. The stock solution of silver nanoclusters was diluted in a solution of PVA (Sigma Aldrich) in MQ water until it reached a concentration of about 10⁻⁸ M. The solution was drop-cast onto an annealed glass coverslip (Menzel) that had been partially covered by self-assembled one micrometer diameter fluorescently labeled carboxylate-modified polystyrene spheres (L4655-1ML, Sigma Aldrich).

Confocal fluorescence microscopy. Images were acquired with a home-built confocal microscope.² We used the output of a pulsed white light laser (SuperK EXTREME EXB-6) which produces a continuous emission spectrum from 420 to 2400 nm. The spectrum was firstly filtered by a 950 nm short-pass filter (Semrock) and a 488 nm long-pass filter (Semrock Razor Edge). The residual spectrum was then separated into a short (primary) and a long (secondary) wavelength part by a tunable long-pass filter (Semrock Versachrome, TLP01-628) which was tilted to transmit light below 570 nm. This short wavelength part was further filtered by a 561 nm bandpass (Semrock MaxLine Laser Line) and a 633 nm short-pass (Semrock). The long wavelength part, serving as secondary excitation laser, was reduced to the wavelength region between 765 and 850 nm with a bandpass filter (Chroma ET810/90M) and sent through a delay line, resulting in a constant time delay of $\delta t = 27$ ns (Figure S11) or 40 ns (Figure 1 and 2) with respect to the primary

excitation pulse. Both beams were coaligned by transmission/reflection through a second tunable long-pass filter (Semrock Versachrome, TLP01-628) and then reflected by a 30:70 beam splitter (XF122 Omega Optical) into an oil immersion objective (Olympus, UPlanSApo 100 \times , NA=1.4). The fluorescence signal was collected with the same objective. Primary and secondary laser light was blocked by a 561 nm long-pass filter (Semrock Edge Basic) and a 700 nm short-pass filter (Chroma, ET700SP-2P8). The fluorescence signal was then detected by an avalanche photodiode (Perkin-Elmer CD3226) connected to a single photon counting module (Becker & Hickl SPC-830). Recording of spectra was achieved by sending the fluorescence signal to a liquid nitrogen-cooled spectrograph (Princeton Instruments SPEC-10:100B/LN_eXcelon CCD camera, SP 2356 spectrometer, 300 grooves/mm). Data were analyzed with self-written Matlab algorithms.

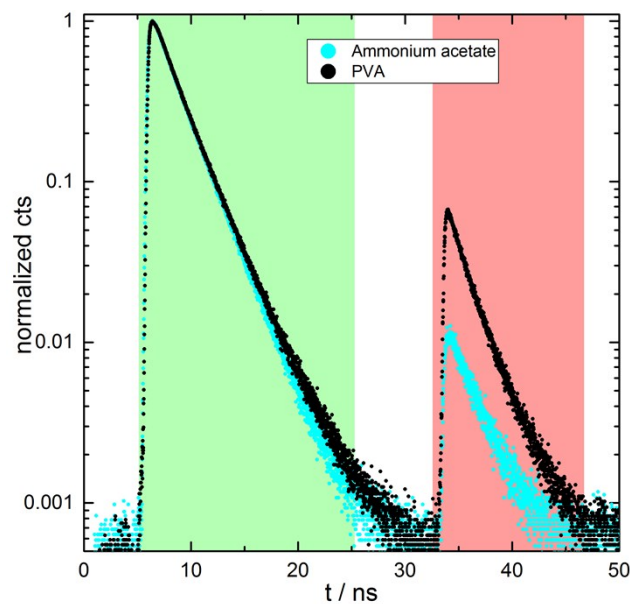


Figure S11: Fluorescence decay curves (first decay after excitation with 560 nm) and optically activated delayed fluorescence decay curves (second decay after illumination with 765 - 850 nm) for an ensemble of DNA-AgNCs in a 10 mM ammonium acetate solution (light blue) and embedded in PVA (black). Primary and secondary excitation intensities were 3.7 kW/cm² and 85 kW/cm², respectively.

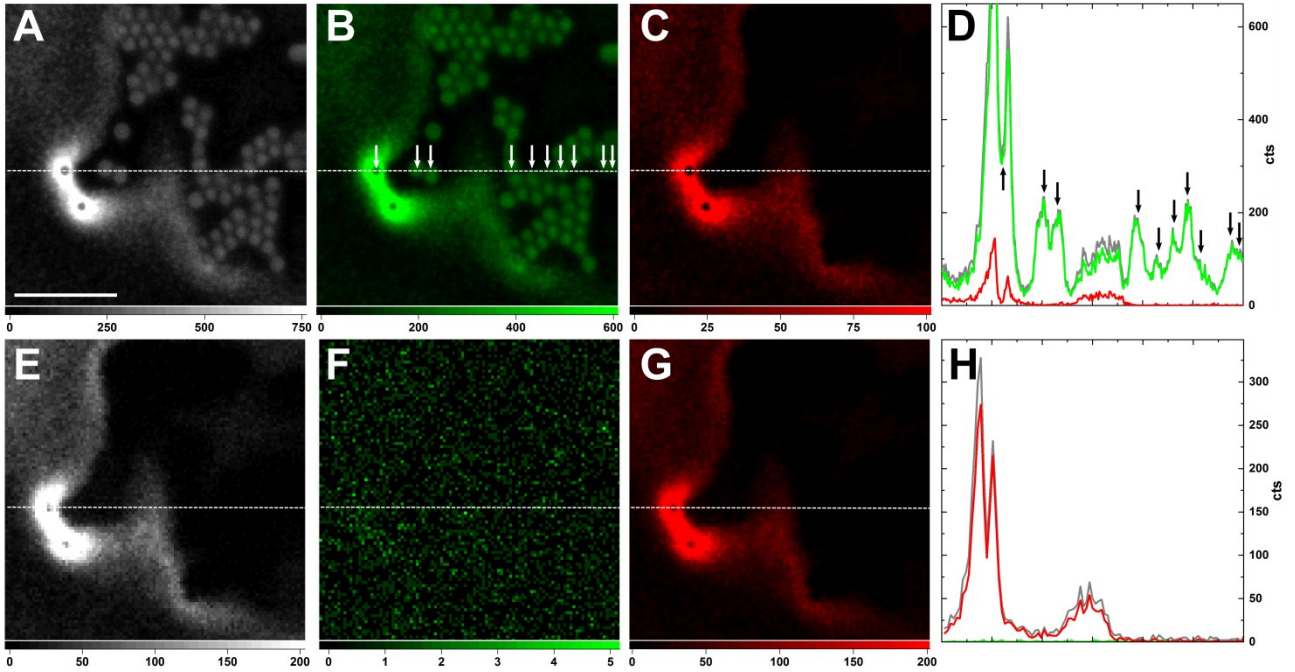


Figure S12: **A)** Fluorescence image of a heterogeneous sample of fluorescently-labeled polystyrene microspheres and PVA-embedded DNA-AgNCs. The image was reconstructed using photons from both primary and secondary laser excitation (0-65 ns). The scale bar corresponds to 10 μm . **B)** and **C)** Same as **(A)** using only the primary (7-17 ns) **(B)** or secondary (46-55 ns, OADF) **(C)** fluorescence signal for image reconstruction. White arrows in **(B)** mark positions of fluorescent beads situated on the white dashed cross-section line, which is shown in **(A)**, **(B)** and **(C)**. **D)** Intensity profiles of the cross-section lines in the previous images **(A)**, **(B)** and **(C)**. The colors are chosen according to the image colors. Black arrows indicate the position of the spheres pointed out in **(B)**. **E)** Fluorescence image of the same sample area applying exclusively the secondary excitation laser 765 - 850 nm (0-65 ns). **F)** and **G)** Same as **(E)** using only the micro-time range for primary (7-17 ns) **(F)** and secondary (46-55 ns, UCF) **(G)** fluorescence. **H)** Intensity profiles of the cross-section lines in the previous images **(E)**, **(F)** and **(G)**. The colors are chosen according to the image colors.

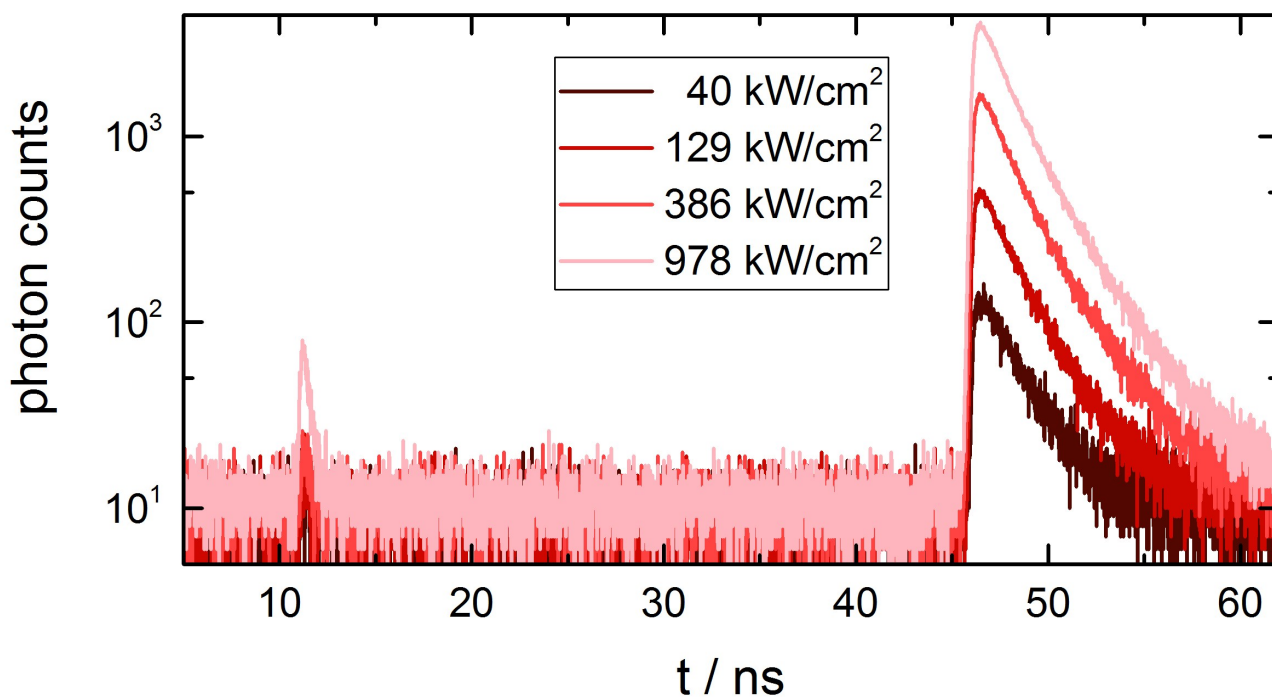


Figure SI3: UCF decay curves (decay after illumination with 765-850 nm) for an ensemble of DNA-AgNCs embedded in PVA at different excitation intensities.

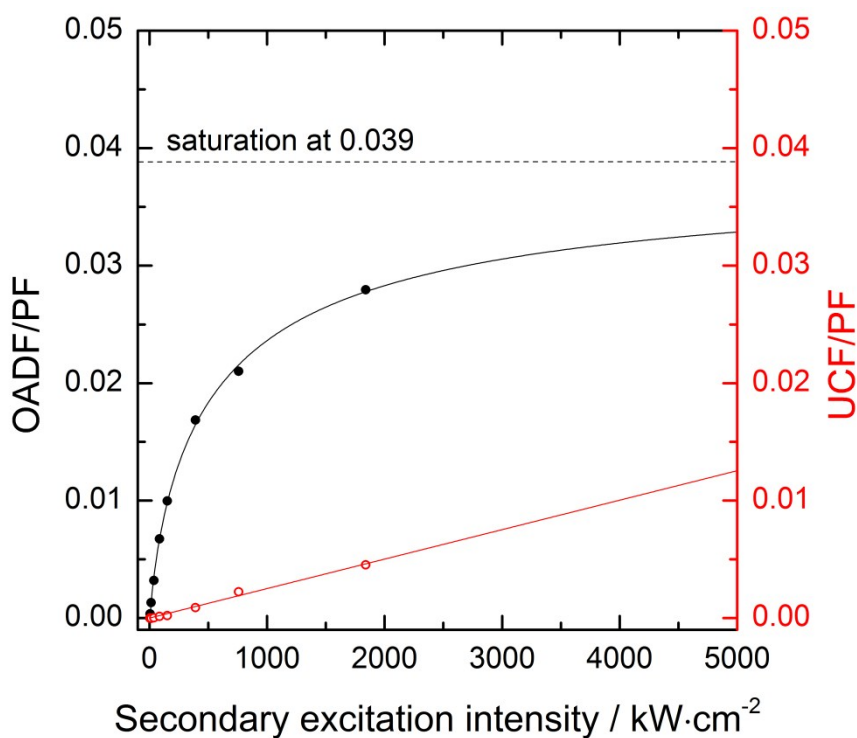


Figure SI4: OADF/PF (black data) and UCF/PF (red data) ratios of the red emitting DNA-AgNCs in a 10 mM ammonium acetate solution. Primary

excitation intensity was 3.7 kW/cm^2 , similar as in Figure SI1. The signal in the red channel in Figure SI1 is the sum of OADF and UCF. To determine the UCF contribution from the sum signal in the red channel, the primary excitation beam was blocked. This allows disentangling the contribution of OADF and UCF to the red channel.

Estimation of Q_{D1} in solution.

The quantum yield of fluorescence Q , upon primary excitation only, in solution is 0.8 at 25°C .¹ Therefore, by definition, Q_{D1} cannot be more than $1 - Q = 0.2$. This establishes an upper boundary for the value of Q_{D1} . Q can also be written as $Q = Q_{S1} \cdot Q_F$ (Q_{S1} is the quantum yield of S1 formation upon primary excitation and Q_F is the quantum yield of fluorescence from S1 to S0). The lower boundary can be established from the data in Figure SI4. In the condition that we use, a secondary excitation intensity that would depopulate all created dark states from the primary excitation, a maximum OADF/PF ratio of 0.039 would be possible. Assuming similar photophysical properties of the OADF and PF emission (decay time and Q_F) we can use this ratio to estimate how much of the molecules ended up in the D1 state versus S1 state upon primary excitation. For this we also assume that the quantum yield for going from D1 to S1 (Q_{D1-S1}) in the OADF process is 1. Hence, 0.039 will then form the lower boundary. In case Q_{D1-S1} is below 1, the actual Q_{D1} will be higher than 0.039 (but can't exceed 0.2 as explained above). Hence Q_{D1} can be estimated to be between 0.039 and 0.2.

1. Cerretani, C.; Carro-Temboury, M. R.; Krause, S.; Bogh, S. A.; Vosch, T., Temperature dependent excited state relaxation of a red emitting DNA-templated silver nanocluster. *Chem. Commun.* **2017**.
2. Liao, Z.; Hooley, E. N.; Chen, L.; Stappert, S.; Müllen, K.; Vosch, T., Green Emitting Photoproducts from Terrylene Diimide after Red Illumination. *J. Am. Chem. Soc.* **2013**, *135* (51), 19180-19185.